ACS OMEGA

Open Access

http://pubs.acs.org/journal/acsodf

Article

Amine-Decorated Methacrylic Acid-based Inverse Vulcanized Polysulfide for Effective Mercury Removal from Wastewater

Ali Shaan Manzoor Ghumman, Rashid Shamsuddin,* Zeid A. Alothman,* Ammara Waheed, Ahmed M. Aljuwayid, Rabia Sabir, Amin Abbasi, and Abdul Sami

Cite This: *ACS Omega* 2024, 9, 4831−4840

Read Online

ACCESS | Metrics & More | Article Recommendations | Supporting Information

ABSTRACT: Mercury [Hg(II)] contamination is an indefatigable global hazard that causes severe permanent damage to human health. Extensive research has been carried out to produce mercury adsorbents; however, they still face certain challenges, limiting their upscaling. Herein, we report the synthesis of a novel amine-impregnated inverse vulcanized copolymer for effective mercury removal. Poly(S-MA) was prepared using sulfur and methacrylic acid employing the inverse vulcanization method, followed by functionalization. The polyethylenimine (PEI) was impregnated on poly(S-MA) to increase the adsorption active sites. The adsorbent was then characterized byusing Fourier transform infrared (FTIR) spectroscopy and scanning electron microscopy (SEM). FTIR spectroscopy confirmed the formation of the copolymer, and successful impregnation of PEI and SEM revealed the composite porous morphology of the copolymer. Amine-impregnated copolymer [amine@poly(S-MA)] outperformed poly(S-MA) in mercury as it showed 20% superior performance with 44.7 mg/g of mercury adsorption capacity. The adsorption data best fit the pseudo-second-order, indicating that chemisorption is the most effective mechanism, in this case, indicating the involvement of NH_2 in mercury removal. The adsorption is mainly a monolayer on a homogeneous surface as indicated by the 0.76 value of Redlich-Peterson exponent (g), which describes the adsorption nature advent from the R^2 value of 0.99.

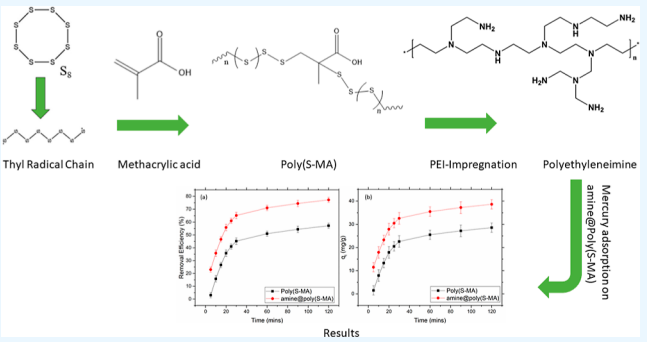

INTRODUCTION

Water contamination has become a severe threat to the public health and environment on planet Earth. In addition to causing immediate health effects such as nausea, vomiting, and diarrhea, water contamination can have long-term consequences such as cancer, reproductive problems, and developmental delays.[1,2] Among various water pollution resources, heavy metals are the most significant because they are toxic even at low concentrations and nonbiodegradable. Moreover, heavy metals can accumulate in the food chain in plants and fish. Agricultural and industrial activities primarily generate heavy metal-containing wastewater. Industries such as mineral processing, leather tanneries, textile dyes, petroleum refineries, and electroplating often emit large quantities of wastewater exceeding the permissible limit set by the World Health Organization (WHO).[3] Effective management of heavy metal pollution in water requires a comprehensive approach that involves monitoring, regulation, and prevention measures.

Mercury (Hg) is among the top five most toxic heavy metals of concern by WHO, and its emission to the environment from anthropogenic sources was estimated to be 2200 tons in 2015.[4] Anthropogenic sources include fossil fuel burning (24% specifically coal), the iron and steel industry, cement production, metal smelting, artisanal gold mining,[5] chloralkali industry, and waste disposal.[6] Mercury ion (Hg^{2+}) is significantly toxic and can cause damage to kidneys and lungs, while methylmercury (organic form) consumption can result in severe brain dysfunction issues. As it is non-biodegradable, the only solution to the mercury pollution problem is its removal or immobilization in the environment.

Mercury eradication from wastewater can be achieved via numerous techniques, including ion exchange, membrane separation, electrochemical treatment, chemical precipitation, adsorption, coagulation, flocculation, and membrane separation.[7,8] Despite the availability of various methods/techniques to remove mercury and other heavy metals from water, most of these techniques cannot be used commercially due to their high cost, production of harmful sludge, and low efficiency.[9] Adsorption offers many advantages, such as its excellent

Received: October 24, 2023
Revised: December 15, 2023
Accepted: January 4, 2024
Published: January 17, 2024

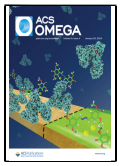

removal efficiency, low cost, abundantly available raw materials, flexibility, and low energy consumption.[9] Therefore, lots of research has been done in this regard, and a wide range of materials, including but not limited to clay, biomass, carbon-based adsorbents, and functionalized silica, have been tested for their adsorption capabilities.[10,11] Nonetheless, certain limitations need to be eliminated if adsorption must be applied on an industrial scale for efficient wastewater treatment; for instance, the adsorbents which have the highest efficiency are either expensive (sulfur-impregnated activated carbon or ion exchange resins) or have low uptake efficiency when manufactured from abundantly available cheap sources (biosorbents).[6] This results in an increased demand to develop low-cost adsorbents with high removal efficiency that are not only able to eradicate ionic mercury Hg(II) but also can be employed on a large scale for the removal of other commonly encountered mercury forms such as organomercury, liquid mercury, inorganic mercury complexed with organic ligands, and mercury vapors.[12]

These efforts to develop an available sorbent that can handle various forms of mercury with high removal efficiency and is made of abundantly available raw materials have been going on for some time. Elemental sulfur is one such raw material produced in excess of 70 million tons per year as a byproduct of the petroleum processing industry.[13] This amount is increasing as more and more sulfur-rich crude oil is now being processed to meet the energy needs of the entire world. Though sulfur can capture and subsequently stabilize mercury,[14] it has some practical constraints like its flammability, inability to mix effectively with wastewater for mercury removal in batch processing, and caking tendency, which could result in high hydraulic pressure drop during filtration. Additionally, it poses a threat to the environment by producing methylmercury, a highly toxic chemical, and it is formed when sulfur is reduced to sulfate by sulfate-reducing bacteria in the soil and sediments.[15]

Recently, much attention has been paid to sulfur polymers synthesized by inverse vulcanization due to many merits of the inverse vulcanization process, which align with greener chemistry approach such as no solvent requirement, flexibility in organic monomer choice, and minimum byproducts. Inverse vulcanized sulfur polymers contain 50−80% sulfur which are synthesized by reacting elemental sulfur and organic monomers.[16] The process is instigated by high temperature (>159 °C) ring opening of S_8 (homolytic scission of S−S bond) generating thiyl diradical which subsequently reacts with either S to form polysulfide or form a C−S bond with unsaturated organic molecules forming polymeric sulfur. The significant difference between inverse vulcanization and the vulcanization process is the sulfur content and its role. In the classic vulcanization process, sulfur acts as a cross-linker, making up only 1−3% of vulcanized rubber.[17,18] While in inverse vulcanization, an unsaturated organic compound in small quantity acts as a cross-linker to form polysulfide polymers with sulfur content ranging from 50 to 80%. These sulfur polymers are promising ways to use abundantly produced petroleum industry waste products in varied application areas such as energy storage LiS batteries, water purification, controlled fertilizer release, nanotechnology, and adhesive material.[18−22] Polysulfides (PS) have a great tendency to remove Hg^{2+} from wastewater due to their high sulfur content, and according to hard−soft acid−base theory (HSAB), sulfur as a soft base has a moderate affinity for soft acid Hg^{2+}.[23] As discussed, polysulfides can be synthesized from the inverse vulcanization process by using various comonomers like waste unsaturated triglycerides,[19,24−27] limonene,[28] diisopropyl benzene,[29] dicyclopentadiene,[30] and myrcene.[31] However, despite their high S content, all these polysulfides (PS) demonstrated poor Hg^{2+} remediation capability and hence cannot be considered for practical applications. Such outcomes require further inspection of the parameters and properties of PS to warrant practical applications. Various efforts have been undertaken to enhance the mercury uptake capacity of the inverse vulcanized copolymers.[32] These include strategies such as coating the inverse vulcanized copolymers onto silica gel surfaces[33,34] and generating fibrous mats through electrospinning. Notably, the electrospun fibrous mats were created by blending the inverse vulcanized copolymers with poly(methyl methacrylate) (PMMA). This innovative approach yielded a remarkable adsorption capacity of 440 mg/g, showcasing the effectiveness of the modified copolymer for mercury removal. Another strategy includes the functionalization of the inverse vulcanized copolymer using *N*-methyl D-glucamine to increase the hydration of the copolymer.[35] However, these strategies increase the overall cost of the adsorbent, limiting their scalabity. Using organic comonomer in inverse vulcanization rendered PS hydrophobic, hence low dispersibility in aqueous media (no hydrogen bond formation).[36] Hg^{2+} ions cannot reach the binding sites due to low wettability, which leads to a low adsorption capacity of PS. This implies that only high sulfur contents cannot guarantee good adsorption affinity. The metal and PS polymer surface interaction also play a critical role.[37]

To overcome the above-stated challenge, hydrophilic PS can be developed by utilizing monomers rich in oxygen-containing functional groups (−OH, −C═O, and −COOH) in an inverse vulcanization process. Recently, hydrophilic polysulfides have been produced by utilizing oxygenous monomers such as methacrylic acid[38] and diallyl dimethylammonium chloride[39] for mercury remediation. However, these polysulfides require blending with polyacrylonitrile and possess low selectivity and uptake capacity.[35]

In inverse vulcanization, it is often convenient for the organic comonomer to have a boiling point higher than the melting point of sulfur, so that the organic monomer is not lost by volatilization. Methacrylic acid is one such acid, which is organically soluble in both water and most organic solvents with a boiling point of 161 °C. Amine containing adsorbents for mercury remediation are in the spotlight due to the promising chelating properties of N atoms. Recently, it has been observed that the adsorption capacity of the silica gel for Hg^{2+} was increased five times by functionalizing the silica gel with amine.[40]

In this study, we prepared a polysulfide-methacrylic acid polymer [poly(S-MA)] by an inverse vulcanization process, which was further impregnated with an amine to introduce more functional groups on the polymer surface that can adsorb Hg^{2+}. Previously no work has been done in this specific category, and this type of polymer is being employed for the first time for Hg^{2+} remediation to the best of our knowledge. Due to a lack of fundamental literature on poly(S-MA), a comprehensive characterization study was carried out to understand the binding mechanism. The adsorption performance of poly(S-MA) was thoroughly evaluated in terms of kinetics, adsorption capacity, and equilibrium isotherms.

https://doi.org/10.1021/acsomega.3c08361
ACS Omega 2024, 9, 4831−4840

EXPERIMENTAL SECTION

Materials. Elemental sulfur (assay 99.9%) and methacrylic acid were procured from PC laboratory reagents, Malaysia and Merck, Malaysia, respectively. Polyethylenimine (PEI) and ethanol were purchased from Sigma-Aldrich, USA.

Synthesis of Poly(S-MA). To produce poly(S-MA), 4 g of sulfur and 8 g of sodium chloride were heated at 180 °C in a 30 mL glass vial using a thermoset oil bath to initiate the ring-opening process of the sulfur under continuous stirring[27,41,42] after which 4 g of methacrylic acid were added in the mixture in a dropwise manner to avoid sudden temperature drop and left the mixture to react for 1 h. After 1 h, the polymer obtained was removed from a glass vial and placed in a conical flask containing 200 mL of deionized water and shaken for 48 h at room temperature at a speed of 220 rpm to remove sodium chloride from the polymer to generate pores followed by overnight drying of the polymer using the oven. After that, the dried polymer was grounded using mortar and pestle. The obtained powdered polymer was used for further experimentation.

Amination of Poly(S-MA). First, a 50/50 vol % polyethylenimine and ethanol mixture was prepared for amine impregnation. Then, poly(S-MA) was placed in an amine solution, followed by continuous shaking for 24 h. After this, the excess liquid was removed from the mixture, and the obtained solid material was used as an adsorbent.

Characterization of Poly(S-MA) and Amine@poly(S-MA). PerkinElmer Frontier spectrometer was used to investigate and compare the chemical composition of poly(S-MA) and amine@poly(S-MA) using attenuated total reflectance with 4 cm^{-1} resolution, eight scan frequency, and 4000−500 cm^{-1} range.

The morphology of both copolymers was investigated using a Zeiss SUPRA 55VP microscope equipped with an INCAx-act EDX Oxford spectroscope.

The specific surface area of poly(S-MA) and amine@poly(S-MA) was evaluated using Brunauer−Emmett−Teller (BET) nitrogen adsorption−desorption isotherms. Isotherms were obtained using Micrometrics Instruments ASAP 2020 at −196 °C. Before surface area analysis, the samples were degassed at 60 °C for 6 h. The Barrett−Joyner−Halenda (BJH) method was also employed to investigate the pore volume and size/dimensions.

Batch Mercury Adsorption Tests. A 1000 ppm mercury chloride stock solution was prepared by dissolving mercury chloride in 1 L of distilled water. Later, this solution was used to prepare various known concentrated solutions for experiments.

An adsorption test was conducted by placing 0.05 g of the copolymer in 50 mL of mercury-contaminated water with an initial concentration of 50 ppm in a 250 mL conical flask. The mixture was then placed in an incubator shaker for a desired time at 220 rpm speed, pH 6, and room temperature. The pH of the mercury solution in all experiments was maintained at 6, as the maximum adsorption capacity was achieved at this pH in our preliminary experiments. After the desired time, the mixture was removed from the shaker and the treated solution was analyzed. Using the calibration curve method, the cold vapor-atomic absorption method was utilized to evaluate the mercury concentration of water samples. The calibration curve for mercury was first obtained using an Agilent model 65 CV-AA using a conventional hollow cathode lamp. The empirical equation from the calibration curve was then used to calculate the mercury concentration by measuring light absorbance using the CV-AA of the treated solution.

Removal efficiency and mercury adsorption capacity of the developed copolymer can be calculated using eqs 1 and 2

$$\text{removal efficiency } (\%) = \frac{C_o - C_e}{C_0} \times 100 \tag{1}$$

$$q_e \text{ (mg/g)} = \frac{C_o - C_e}{W} \times V \tag{2}$$

In which initial and equilibrium mercury concentrations are represented by C_o (mg/L) and C_e (mg/L) in each solution, respectively. W (g) and V (L) are the weights of the dry adsorbent and the volumes of the solution, respectively.

Equilibrium Isotherms and Kinetics. *Equilibrium Isotherms.* To investigate the equilibrium isotherm for mercury adsorption using amine-functionalized copolymer, batch adsorption experiments were conducted at different initial mercury concentrations, keeping other parameters fixed. To carry out this, 0.05 g of amine@poly(S-MA) was placed in 50 mL of mercury solution with different initial concentrations (i.e., 10, 20, 30, 40, and 50) in a 250 mL conical flask, and the pH was maintained at 6. The solution was stirred at 220 rpm for 3 h at room temperature by using an incubator shaker. The remaining mercury concentration was measured by using CV-AA.

Three well-known isotherm adsorption models, including Langmuir, Freundlich, and Redlich-Peterson (in their nonlinear form), were fitted to the obtained adsorption data from varying initial concentrations to investigate the adsorption nature of amine@poly(S-MA).

Langmuir Isotherm. Equation 3 represents the Langmuir isotherm model. This isotherm explains the monolayer adsorption without lateral interactions assuming the homogeneous flat surface of the adsorbent with similar binding sites and adsorbates behave ideally.

$$q_e = \frac{Q_L K_L C_e}{1 + K_L C_e} \tag{3}$$

where q_e (mg/g) and C_e (mg/L) are mercury concentration and adsorption capacity at equilibrium, respectively, and Q_L (maximum adsorption capacity, mg/g) and K_L (mass transfer coefficient, L/mg) are Langmuir adsorption constants.

Freundlich Isotherm. Equation 4 depicts the Freundlich isotherm model, which explains multilayer adsorption, unlike Langmuir isotherm on the heterogeneous adsorbent surface with nonuniform adsorption heat.

$$q_e = K_F C_e^{1/n} \tag{4}$$

where q_e (mg/g) and C_e (mg/L) are the mercury concentration and adsorption capacity at equilibrium, respectively, and KF (mg/g) $(L/mg)^{(1/n)}$ is the adsorption constant. In contrast, n is the heterogeneity factor showing the intensity of adsorption.

Redlich-Peterson Isotherm. Equation 5 shows the Redlich-Peterson isotherm model, which is appropriate for all types of surfaces, either heterogeneous or homogeneous, as it explains the features of both Langmuir and Freundlich isotherms.

$$q_e = \frac{K_R C_e}{1 + A_R C_e^g} \tag{5}$$

https://doi.org/10.1021/acsomega.3c08361
ACS Omega 2024, 9, 4831−4840

where q_e (mg/g) and C_e (mg/L) are the mercury concentration and adsorption capacity at equilibrium, respectively. A_R (L/mg) and K_R (L/g) are model constants, whereas g is the exponential factor.

Kinetics of Mercury Adsorption. To investigate the Kinetics of mercury adsorption, a batch adsorption test was carried out with 50 ppm initial mercury concentration and different adsorption times while fixing other parameters. To do this, 0.05 g of amine@poly(S-MA) was placed in a 50 mL mercury solution with 50 ppm initial concentration in a 250 mL conical flask, and the pH was maintained at 6. The solution was stirred at 220 rpm for a specific time ranging from 5 to 300 min at room temperature using an incubator shaker. The remaining mercury concentration was measured using CV-AA. Nonlinear forms of pseudo-first- and second-order kinetic models were fitted to the obtained adsorption kinetic data. In almost every case, either model can explain the adsorption kinetics.

Pseudo-First Order. Equation 6 depicts the pseudo-first-order kinetic model, which assumes that physisorption dominates the chemisorption, and the rate of adsorption increases with the number of vacant active sites.

$$q_t = q_e(1 - e^{-k_1 t}) \tag{6}$$

q_t is the amount of mercury adsorbed at t time, q_e (mg/g) is mercury adsorption capacity at equilibrium, and K_1 (1/min) is the rate constant.

Pseudo-Second Order. Equation 7 shows a pseudo-second-order model which assumes chemical absorption dominated physisorption and the adsorption rate is directly proportional to the square of the number of vacant active sites.

$$q_t = \frac{K_2 q_e^2 t}{1 + K_2 q_e t} \tag{7}$$

q_t is the amount of mercury adsorbed at t time, q_e (mg/g) is the mercury adsorption capacity at equilibrium, and K_1 (1/min) is the rate constant.

RESULTS AND DISCUSSION

Fourier Transform Infrared Spectroscopy. Figure 1 depicts the Fourier transform infrared (FTIR) spectra of poly(S-MA) and amine-impregnated poly(S-MA). The spectrum of poly(S-MA) shows stretching signals for C−S (660 cm^{-1}), C═O (1695 cm^{-1}), −OH (3341 cm^{-1}), and C−O (1116 cm^{-1}). No signal appeared for the C═C stretching at 1640 cm^{-1}. The appearance of signals for C−S and the disappearance of C═C in the spectrum of poly(S-MA) confirms the successful formation of the sulfur-methacrylic acid copolymer [poly(S-MA)]. Here, the material formed as a result of the alkene reaction is hypothesized to be a polymer, as the resultant material is insoluble in most of the organic solvents (such as chloroform, tetrahydrofuran, benzene, toluene, etc.) (shown in Figure S1), which limits its characterization using H NMR and GPC to confirm the polymer formation. The spectrum of amine@poly(S-MA) shows similar signals as appeared in the case of poly(S-MA), except a few new signals appeared at 3284, 1563, 1452, and 1045 cm^{-1} these represent N−H stretching, symmetric NH_2 bending, asymmetric NH_2 bending, and C−N (secondary amine) stretching vibrations, respectively. The appearance of these peaks confirms the successful impregnation of the amine on the developed copolymer, which is indispensable for mercury adsorption. Moreover, the Raman spectrum shown in Figure S2 also confirms the utilization of the C═C bond and the appearance of C−S bonds.

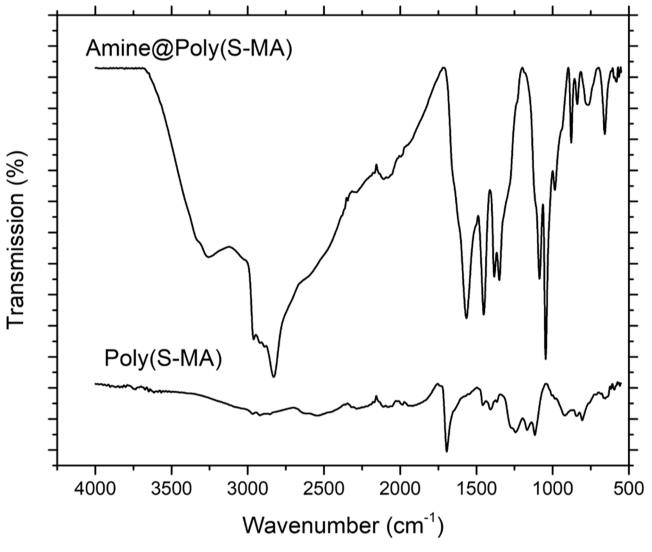

Figure 1. FTIR spectra of poly(S-MA) and amine@poly(S-MA).

Thermal Properties of the Polymer. Figure 2 illustrates the thermal stability of the developed adsorbents. The

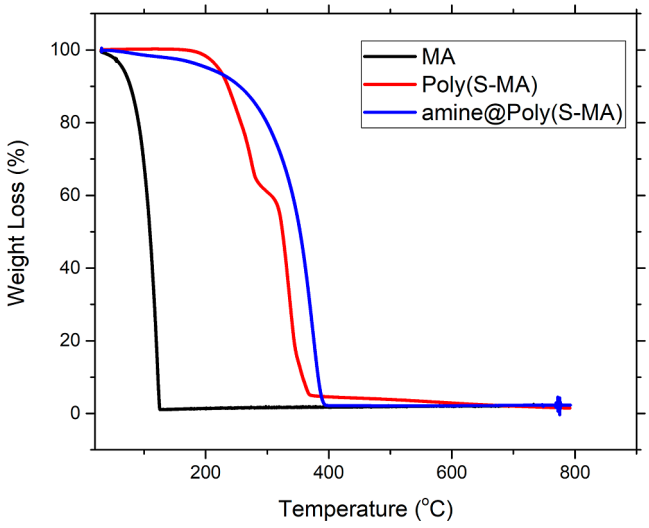

Figure 2. TGA Thermogram of methacrylic acid, poly(S-MA), and amine@poly(S-MA).

methacrylic acid onset degrades at 60 °C and completely degrades at 130 °C. Nevertheless, the hypothesized copolymer produced through the reaction of sulfur and methacrylic acid starts to degrade at higher temperatures (around 200 °C), which shows that the produced copolymer is thermally stable. The poly(S-MA) degrades in two steps. In the first step, the loosely bonded S−S chain and unreacted sulfur degrade, whereas in the second step, the strongly bonded C−S and other organic bonds degrade. The pattern of the degradation and onset temperature changes shows that the hypothesized copolymer has formed.[41,42] DSC thermogram of the copolymer produced is depicted in Figure S3, which shows that the copolymer formed contains the unreacted sulfur as demonstrated by the appearance of the melting peak in the

https://doi.org/10.1021/acsomega.3c08361
ACS Omega 2024, 9, 4831−4840

thermogram at around 112 °C. The percentage of the unreacted sulfur was estimated to be around 9%. The estimation by done using the method explained by Ghumman et al.[42]

Scanning Electron Microscopy. Figure 3 shows scanning electron microscopy (SEM) images for the prepared poly(S-MA) adsorbent. When the magnification is 200× in Figure 3A, plenty of holes and pores are shown on the surface of the adsorbent. When zooming into 5000× in Figure 3B, a lot of pores can be seen clearly, but there are some granular particles around the pores, which is unreacted sulfur. Figure 3D at 5000× magnification also shows that many pores are available on the adsorbent surface. This is because sodium chloride (NaCl) was initially combined with a polymer; when it dissolved in water during the purification process, the initial NaCl spot became empty, increasing the porosity and surface area of the adsorbent.

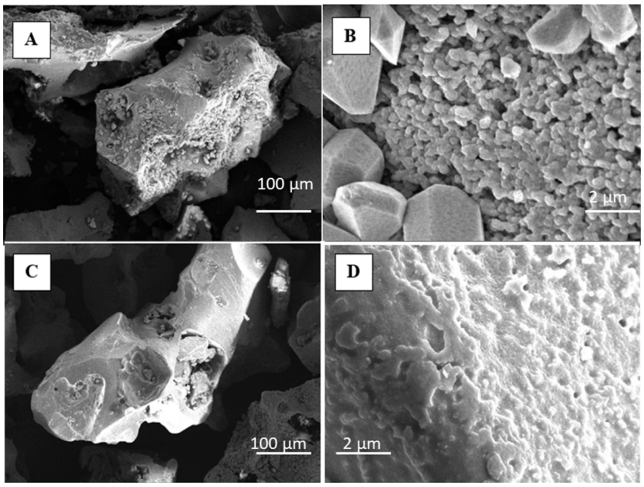

Figure 3. SEM images of poly(S-MA): (A) at 200× magnification, (B) at 5kx magnification, (C) at 200× magnification, and (D) at 5kx magnification.

Figure 4 shows SEM images of the amine-impregnated poly(S-MA) adsorbent. The condition of amine polymer is like sticky mud where the powder form of poly(S-MA) is mixed with a liquid form of polyethylenimine during amination. Figure 4A, which is 100× magnification, shows that the amount of pores decreased because the amine is impregnated successfully onto poly(S-MA). The holes and pores on the poly(S-MA) surface have been filled with amine.

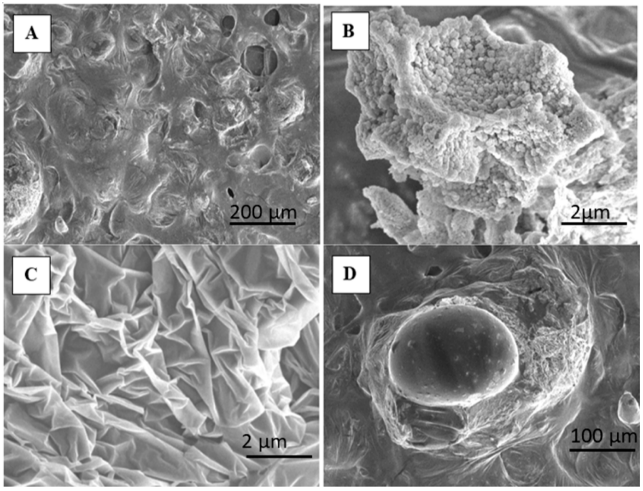

Figure 4. SEM images of amine impregnated poly(S-MA) (A) at 100× magnification, (B) at 5kx magnification, (C) at 5× magnification, and (D) at 200× magnification.

Table 1 shows the analysis data of the elemental weight percentage of each of the elements in poly(S-MA) and amine-impregnated poly(S-MA) obtained by the EDX result. Weight percentage of carbon, C for amine-poly(S-MA) has increased from 33.48 wt % from poly(S-MA) to 53.86 wt %. For amine-poly(S-MA) 's nitrogen, N and oxygen, O weight percentages also increase from 3.29 to 15.47 and from 3.29 to 6.34 wt %, respectively, from poly(S-MA). It can be concluded that N−H and −OH functional group is presented higher in the amine polymer that is responsible for mercury adsorption. It shows that amine, which has an N−H bond, is successfully impregnated on poly(S-MA), which increases the N weight percentage.

Table 1. EDX Elemental Weight Percentages of Two Adsorbents

	C	N	O	S
EDX poly(S-MA) (wt %)	33.48	4.78	3.29	58.45
EDX amine impregnated poly(S-MA) (wt %)	53.86	15.47	6.34	24.34

Surface Area. Figure 5 demonstrates the N_2 adsorption−desorption isotherm for the developed copolymer. The summary of surface and pore characteristics is presented in Table 2. The N_2 adsorption−desorption shows trends similar to those of some reported adsorbents. According to IUPAC classification, this isotherm is type III, meaning that the developed adsorbent is nonporous or have macropores.[43] The BJH pore size distribution demonstrated that the developed poly(S-MA) has micropores (<2 nm) structure with some extent of mesoporous structures as it is below 20 nm. Nevertheless, the low BJH surface are of pores is the main disadvantage which could affect mercury adsorption. This is

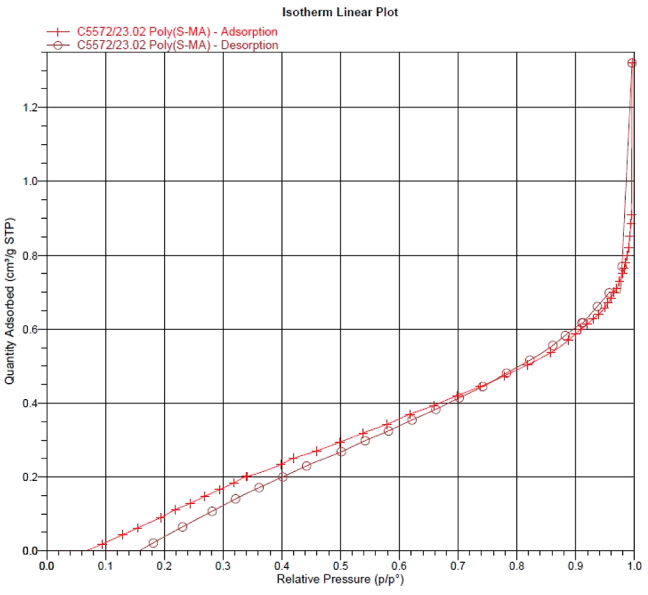

Figure 5. N_2 adsorption−desorption isotherm of poly(S-MA).

https://doi.org/10.1021/acsomega.3c08361
ACS Omega 2024, 9, 4831−4840

Table 2. Surface Area and Pore Characteristic of Poly(S-MA)

sample	BET surface area (m^2/g)	BJH pore volume (cm^3/g)	BJH average pore size (nm)	BJH surface area of pores (m^2/g)
poly(S-MA)	1.60	0.00194	9.378	0.756
amine@poly(S-MA)	0.193	0.000836	69.2	0.034

the reason we tend to functionalize the material with amine to compensate the low surface area. The surface area of the adsorbent reduces from 1.6 to 0.193 m^2/g after impregnating PEI onto the poly(S-MA), which is because the amine covers the pores which reduces the number of pores available.

Batch Adsorption. Figure 6 shows the mercury adsorption performance of both poly(S-MA) and amine@poly(S-MA). The amount of mercury removed increases as time passes in both cases. However, amine@poly(S-MA) outperformed poly(S_MA) in mercury adsorption, as it has shown 20% better adsorption capacity. This is because amine@poly(S-MA) contains an NH_2 functional group that is available for mercury binding, increasing the overall number of active sites for mercury removal.

To further investigate the performance of the amine@poly(S-MA) isotherm, kinetic experiments were analyzed, which are explained in the following sections.

Effect of Amine Concentration. Figure 7 depicts the effect of the amine concentration on the mercury adsorption capacity. The figure demonstrates that the adsorption capacity of the amine@poly(S-MA) increases with the increase in amine concentration. The amine concentration here means the concentration of polyethylenimine (PEI) in an impregnation solution obtained by dissolving PEI in ethanol. The adsorption capacity increases due to the increase in the available active sites in the polymer structures as the amine content increases. The polymer impregnated with 50 wt % concentrated amine solution showed an adsorption capacity of 28.2 mg/g, which is far better than pristine polymer, and this uptake capacity increases to 38.6 mg/g with 100 wt % PEI.

Effect of pH. Figure 8 illustrates the correlation between the pH of the model wastewater and the adsorption of mercury. With an initial mercury concentration of 50 ppm, the percentage of Hg^{2+} removed increases from 46.6 to 77.2% as the pH rises from 2 to 6. However, beyond a pH of 6, the

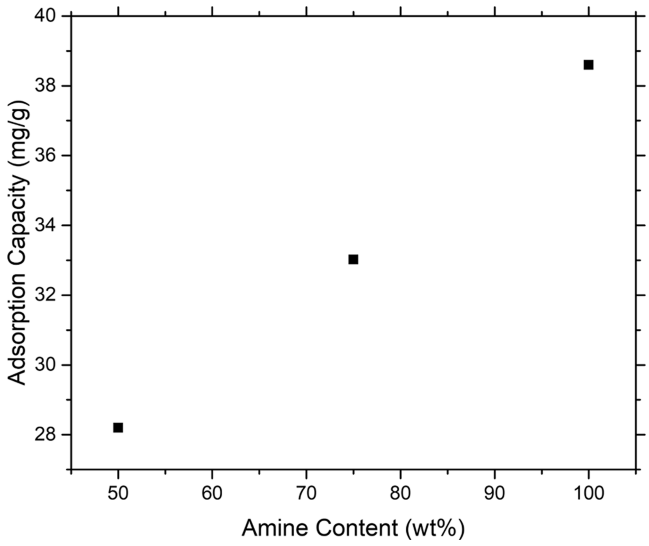

Figure 7. Effect of the amine concentration on adsorption capacity.

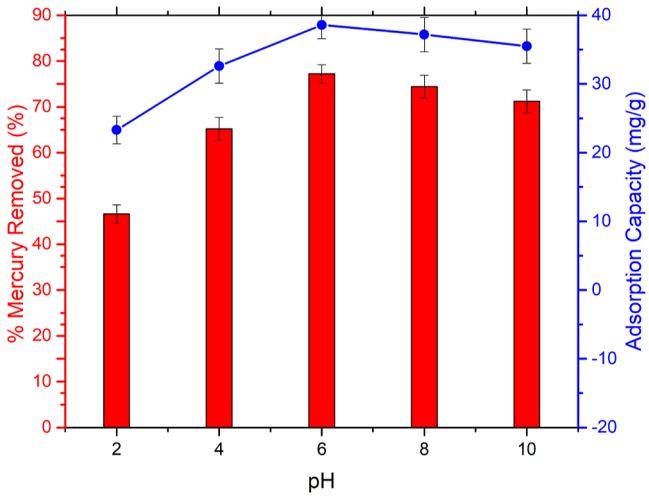

Figure 8. Effect of pH.

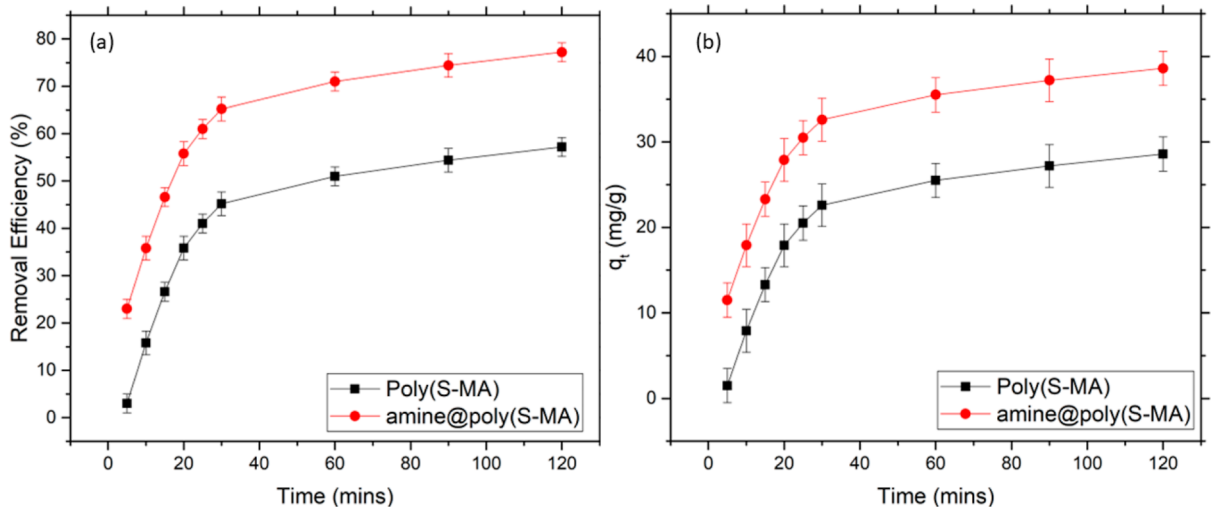

Figure 6. Comparison of mercury (a) removal % and (b) adsorption capacity using poly(S-MA) and amine@poly(S-MA).

https://doi.org/10.1021/acsomega.3c08361
ACS Omega 2024, 9, 4831−4840

removal percentage begins to decline, reaching 71.2% at a pH of 10. According to the mercury speciation diagram, Hg mainly exists as $HgCl_2$ at pH ≤ 6 and as HgO at pH > 6. Additionally, the zeta potential analysis at pH = 6 indicates a negative charge on amine@poly(S-MA), suggesting that the electrostatic attraction between $HgCl_2$ and the amine group in the developed adsorbent could be a key factor contributing to the high removal percentage at pH = 6. The maximum adsorbent capacity of 38.6 mg/g was also observed at pH = 6.

Equilibrium Isotherm of Mercury Adsorption. As explained early, Mercury adsorption data with initial mercury concentration ranging from 10 to 50 ppm while keeping other parameters constant was fitted to the Langmuir, Freundlich, and Redlich-Peterson isotherm model to understand the nature of adsorption. Figure 9 shows the plotted isotherms

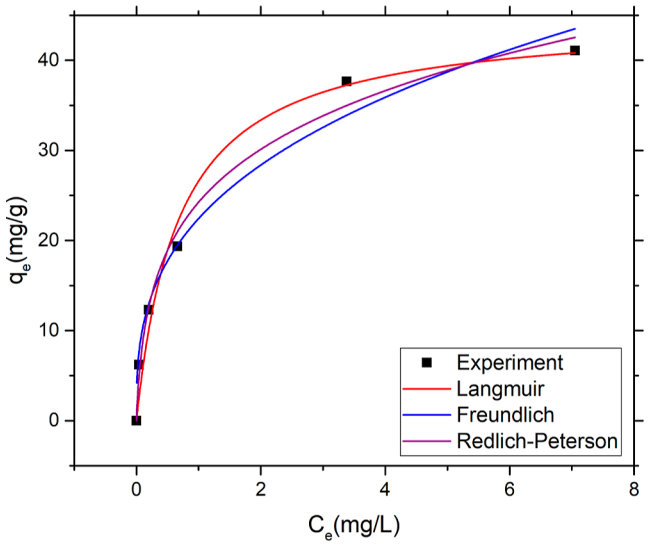

Figure 9. Langmuir, Freundlich, and Redlich-Peterson isotherm plotted for mercury adsorption using amine@poly(S_MA).

for mercury adsorption using above stated models. Table 3 presents the coefficient of determination and other model parameters obtained by nonlinear regression of the adsorption data using the above three models.

High R^2 values of 0.976, 0.982, and 0.99 for Freundlich, Langmuir and Redlich-Peterson, respectively, show that all three models can describe the adsorption data. Nevertheless, Redlich-Peterson has shown the highest value, which demonstrates that the adsorption data have characteristics of both Langmuir and Freundlich isotherms. In simple words, the adsorption of mercury on amine@poly(S-MA) obeys the principle of both monolayer (adsorption on a homogeneous surface) and multilayer (adsorption on a heterogeneous surface). The value of the isotherm exponent of the Redlich-Peterson model is 0.76, which shows that it deviates from the Langmuir model.

The maximum adsorption capacity (monolayer) of the amine@poly(S-MA) is 44.7 mg/g, estimated using the Langmuir model, which is far better as compared to other inverse vulcanized copolymers utilized as mercury adsorbents.[29,30]

Kinetics of Mercury Adsorption. Figure 10 depicts the plotted pseudo-first-order and pseudo-second-order kinetic models fitted to the mercury adsorption kinetic data. Table 4 summarizes the parameter of the model obtained by nonlinear regression of the experimental data.

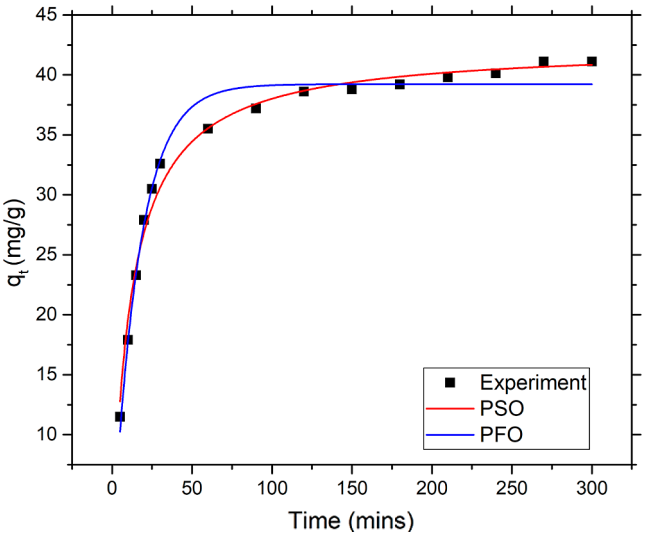

Figure 10. Pseudo first order (PFO) and second kinetic model fitted to mercury adsorption data.

Table 3. Mercury Adsorption Isotherm Parameters

isotherm model	parameters	
Langmuir	R^2	0.982
	Q_L (mg/g)	44.7
	K_L (L/mg)	1.46
Freundlich	R^2	0.976
	K_F (mg/g)(L/mg)$^{1/n}$	22.43
	N	0.339
Redlich-Peterson	R^2	0.990
	A_R (L/mg)	6.6
	K_R (L/g)	185.9
	G	0.76

Table 4. Kinetic Parameters for Mercury Adsorption

kinetic model	parameter	
PFO	R^2	0.98
	K_1 (min^{-1})	0.0605
	q_e (mg/g)	39.22
	error (%)	4.57
PSO	R^2	0.99
	K_2 (min^{-1})	0.00203
	q_e (mg/g)	42.42
	error (%)	3.11

The pseudo-second-order model best fits the experimentation data as it has demonstrated a high R^2 value of 0.99 and low % error, demonstrating that the chemisorption mechanism chiefly controls the adsorption.

At the start, mercury adsorption increases rapidly. However, as time passes, the pace of the increase of adsorption slows down. This is because, at the start of adsorption, more binding sites are available for mercury adsorption, but these sites get occupied with time, reducing the number of active sites for mercury and consequently reducing the rate of adsorption. The equilibrium was achieved after 300 min.

https://doi.org/10.1021/acsomega.3c08361
ACS Omega 2024, 9, 4831−4840

Reusability of the Amine@poly(S-MA). The stability assessment of amine@poly(S-MA) was carried out by submerging it in a 6 M HCl solution, followed by a subsequent test for BaSO4 precipitation. The precipitation examination yielded no evidence of S^{2-} presence, as no precipitates formed, confirming the durability of the adsorbent in the HCl solution. Figure 11 illustrates the impact of the regeneration cycle on the

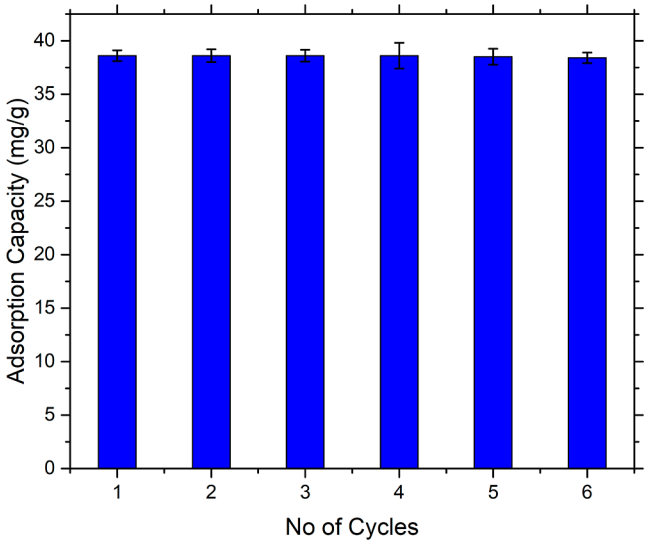

Figure 11. Effect of regeneration cycles on the adsorption capacity.

mercury adsorption capacity of amine@poly(S-MA). The cycling test, involving adsorption and desorption, demonstrated consistent adsorption capacity, with only a slight decrease observed after the sixth cycle, going from 38.6 to 38.4 mg Hg^{2+}/g. Collectively, the adsorption/desorption and precipitation tests underscore the stable performance and potential of amine@poly(S-MA) as a mercury adsorbent suitable for practical applications.

CONCLUSIONS

The successful synthesis of the mercury adsorbent was presented. Poly(S-MA) removed almost 57% mercury within 2 h, increasing to 78% by impregnating the copolymer with amine. The amine-impregnated copolymer showed 20% superior mercury removal performance compared to that of pristine poly(S-MA). Amine@poly(S-MA) showed a tremendously high adsorption capacity of 44.7 mg/g, showing its potential for mercury removal. Moreover, the adsorbent has been prepared using petrochemical industry waste, which makes this adsorbent a sustainable material with promising results.

ASSOCIATED CONTENT

Supporting Information

The Supporting Information is available free of charge at https://pubs.acs.org/doi/10.1021/acsomega.3c08361.

Solubility of the produced polymer, Raman Spectrum of the produced polymer, and DSC thermogram of the all polymers (PDF)

AUTHOR INFORMATION

Corresponding Authors

Rashid Shamsuddin − *Chemical Engineering Department, Universiti Teknologi PETRONAS, Bandar Seri Iskandar 32610 Perak Darul Ridzuan, Malaysia; HICoE, Centre for Biofuel and Biochemical Research (CBBR), Institute of Self-Sustainable Building, Universiti Teknologi PETRONAS, Seri Iskandar 32610 Perak, Malaysia;* orcid.org/0000-0002-8683-596X; Email: mrashids@utp.edu.my

Zeid A. Alothman − *Department of Chemistry, College of Science, King Saud University, Riyadh 11451, Saudi Arabia;* orcid.org/0000-0001-9970-2480; Email: zaothman@ksu.edu.sa

Authors

Ali Shaan Manzoor Ghumman − *Chemical Engineering Department, Universiti Teknologi PETRONAS, Bandar Seri Iskandar 32610 Perak Darul Ridzuan, Malaysia; HICoE, Centre for Biofuel and Biochemical Research (CBBR), Institute of Self-Sustainable Building, Universiti Teknologi PETRONAS, Seri Iskandar 32610 Perak, Malaysia;* orcid.org/0000-0002-3239-9250

Ammara Waheed − *Department of Chemical Engineering, Wah Engineering College, University of Wah, Wah Cantt 47040 Punjab, Pakistan*

Ahmed M. Aljuwayid − *Department of Chemistry, College of Science, King Saud University, Riyadh 11451, Saudi Arabia*

Rabia Sabir − *Department of Chemical Engineering, Wah Engineering College, University of Wah, Wah Cantt 47040 Punjab, Pakistan*

Amin Abbasi − *Technology University of the Shannon (TUS), Athlone N37 HD68, Ireland*

Abdul Sami − *Chemical Engineering Department, Universiti Teknologi PETRONAS, Bandar Seri Iskandar 32610 Perak Darul Ridzuan, Malaysia*

Complete contact information is available at: https://pubs.acs.org/10.1021/acsomega.3c08361

Notes

The authors declare no competing financial interest.

ACKNOWLEDGMENTS

Authors are grateful to the Researchers Supporting Project no. (RSP2024R1), King Saud University, Riyadh, Saudi Arabia. Authors also acknowledge the research funding from ICRF (UTP-Kyutech) (015ME0-314).

REFERENCES

(1) Alharbi, N. S.; Hu, B.; Hayat, T.; Rabah, S. O.; Alsaedi, A.; Zhuang, L.; Wang, X. Efficient Elimination of Environmental Pollutants through Sorption-Reduction and Photocatalytic Degradation Using Nanomaterials. *Front. Chem. Sci. Eng.* **2020**, *14* (6), 1124−1135.

(2) Carolin, C. F.; Kumar, P. S.; Saravanan, A.; Joshiba, G. J.; Naushad, M. Efficient Techniques for the Removal of Toxic Heavy Metals from Aquatic Environment: A Review. *J. Environ. Chem. Eng.* **2017**, *5* (3), 2782−2799.

(3) Chalkidis, A.; Jampaiah, D.; Aryana, A.; Wood, C. D.; Hartley, P. G.; Sabri, Y. M.; Bhargava, S. K. Mercury-Bearing Wastes: Sources, Policies and Treatment Technologies for Mercury Recovery and Safe Disposal. *J. Environ. Manage.* **2020**, *270*, 110945.

(4) Cotruvo, J. A. 2017 WHO Guidelines for Drinking Water Quality: First Addendum to the Fourth Edition. *J. Am. Water Works Assoc.* **2017**, *109* (7), 44−51.

(5) Esdaile, L. J.; Chalker, J. M. Frontispiece: The Mercury Problem in Artisanal and Small-Scale Gold Mining. *Chem.—Eur. J.* **2018**, *24*, 12.
(6) Wang, L.; Hou, D.; Cao, Y.; Ok, Y. S.; Tack, F. M. G.; Rinklebe, J.; O'Connor, D. Remediation of Mercury Contaminated Soil, Water, and Air: A Review of Emerging Materials and Innovative Technologies. *Environ. Int.* **2020**, *134*, 105281.
(7) Fu, Y.; Yang, C.; Zheng, Y.; Jiang, J.; Sun, Y.; Chen, F.; Hu, J. Sulfur Crosslinked Poly(m-Aminothiophenol)/Potato Starch on Mesoporous Silica for Efficient Hg(II) Removal and Reutilization of Waste Adsorbent as a Catalyst. *J. Mol. Liq.* **2021**, *328*, 115420.
(8) Monier, M.; Abdel-Latif, D. A. Preparation of Cross-Linked Magnetic Chitosan-Phenylthiourea Resin for Adsorption of Hg(II), Cd(II) and Zn(II) Ions from Aqueous Solutions. *J. Hazard. Mater.* **2012**, *209−210*, 240−249.
(9) Long, W.; Yang, C.; Wang, G.; Hu, J. Effective adsorption of Hg(II) ions by new ethylene imine polymer/β-cyclodextrin cross-linked functionalized magnetic composite. *Arab. J. Chem.* **2023**, *16* (2), 104439.
(10) Wang, J.; Feng, X.; Anderson, C. W. N.; Xing, Y.; Shang, L. Remediation of Mercury Contaminated Sites - A Review. *J. Hazard. Mater.* **2012**, *221−222*, 1−18.
(11) Da'na, E. Adsorption of Heavy Metals on Functionalized-Mesoporous Silica: A Review. *Microporous Mesoporous Mater.* **2017**, *247*, 145−157.
(12) Beckers, F.; Rinklebe, J. Cycling of Mercury in the Environment: Sources, Fate, and Human Health Implications: A Review. *Crit. Rev. Environ. Sci. Technol.* **2017**, *47* (9), 693−794.
(13) Kutney, G. *Sulfur. History, Technology, Applications & Industry*, 2nd ed.; Elsevier, 2013.
(14) Lopez-Delgado, A.; Lopez, F. A.; Alguacil, F. J.; Padilla, I.; Guerrero, A. A Microencapsulation Process of Liquid Mercury by Sulfur Polymer Stabilization/Solidification Technology. Part I: Characterization of Materials. *Rev. Metal.* **2012**, *48* (1), 45−57.
(15) Meyer, B. Elemental Sulfur. *Chem. Rev.* **1976**, *76* (3), 367−388.
(16) Park, K. W.; Leitao, E. M. The Link to Polysulfides and Their Applications. *Chem. Commun.* **2021**, *57* (26), 3190−3202.
(17) Orme, K.; Fistrovich, A. H.; Jenkins, C. L. Tailoring Polysulfide Properties through Variations of Inverse Vulcanization. *Macromolecules* **2020**, *53* (21), 9353−9361.
(18) Chalker, J. M.; Worthington, M. J. H.; Lundquist, N. A.; Esdaile, L. J. Synthesis and Applications of Polymers Made by Inverse Vulcanization. *Top. Curr. Chem.* **2019**, *377* (3), 16.
(19) Ghumman, A. S. M.; Shamsuddin, R.; Nasef, M. M.; Yahya, W. Z. N.; Abbasi, A.; Almohamadi, H. Sulfur Enriched Slow-Release Coated Urea Produced from Inverse Vulcanized Copolymer. *Sci. Total Environ.* **2022**, *846*, 157417.
(20) Akay, S.; Kayan, B.; Kalderis, D.; Arslan, M.; Yagci, Y.; Kiskan, B. Poly(Benzoxazine-Co-Sulfur): An Efficient Sorbent for Mercury Removal from Aqueous Solution. *J. Appl. Polym. Sci.* **2017**, *134* (38), 1−11.
(21) Lee, T.; Dirlam, P. T.; Njardarson, J. T.; Glass, R. S.; Pyun, J. Polymerizations with Elemental Sulfur: From Petroleum Refining to Polymeric Materials. *J. Am. Chem. Soc.* **2022**, *144* (1), 5−22.
(22) Worthington, M. J. H.; Kucera, R. L.; Chalker, J. M. Green Chemistry and Polymers Made from Sulfur. *Green Chem.* **2017**, *19* (12), 2748−2761.
(23) Müller, F. G.; Lisboa, L. S.; Chalker, J. M. Inverse Vulcanized Polymers for Sustainable Metal Remediation. *Adv. Sustain. Syst.* **2023**, *7* (5), 2300010.
(24) Worthington, M. J. H.; Kucera, R. L.; Albuquerque, I. S.; Gibson, C. T.; Sibley, A.; Slattery, A. D.; Campbell, J. A.; Alboaiji, S. F. K.; Muller, K. A.; Young, J.; Adamson, N.; Gascooke, J. R.; Jampaiah, D.; Sabri, Y. M.; Bhargava, S. K.; Ippolito, S. J.; Lewis, D. A.; Quinton, J. S.; Ellis, A. V.; Johs, A.; Bernardes, G. J. L.; Chalker, J. M. Laying Waste to Mercury: Inexpensive Sorbents Made from Sulfur and Recycled Cooking Oils. *Chem.—Eur. J.* **2017**, *23* (64), 16219−16230.
(25) Tikoalu, A. D.; Lundquist, N. A.; Chalker, J. M. Mercury Sorbents Made By Inverse Vulcanization of Sustainable Triglycerides: The Plant Oil Structure Influences the Rate of Mercury Removal from Water. *Adv. Sustain. Syst.* **2020**, *4*, 1−9.
(26) Hoefling, A.; Lee, Y. J.; Theato, P. Sulfur-Based Polymer Composites from Vegetable Oils and Elemental Sulfur : A Sustainable Active Material for Li - S Batteries. *Macromol. Chem. Phys.* **2017**, *218*, 1−9.
(27) Ghumman, A. S. M.; Shamsuddin, M. R.; Nasef, M. M.; Yahya, W. Z. N.; Ayoub, M.; Cheah, B.; Abbasi, A. Synthesis and Characterization of Sustainable Inverse Vulcanized Copolymers from Non-Edible Oil. *ChemistrySelect* **2021**, *6* (6), 1180−1190.
(28) Crockett, M. P.; Evans, A. M.; Worthington, M. J. H.; Albuquerque, I. S.; Slattery, A. D.; Gibson, C. T.; Campbell, J. A.; Lewis, D. A.; Bernardes, G. J. L.; Chalker, J. M. Sulfur-Limonene Polysulfide: A Material Synthesized Entirely from Industrial By-Products and Its Use in Removing Toxic Metals from Water and Soil. *Angew. Chem.* **2016**, *128* (5), 1746−1750.
(29) Lee, J.; Lee, S.; Kim, J.; Hanif, Z.; Han, S.; Hong, S.; Yoon, M. H. Solution-Based Sulfur-Polymer Coating on Nanofibrillar Films for Immobilization of Aqueous Mercury Ions. *Bull. Korean Chem. Soc.* **2018**, *39* (1), 84−89.
(30) Parker, D. J.; Jones, H. A.; Petcher, S.; Cervini, L.; Griffin, J. M.; Akhtar, R.; Hasell, T. Low Cost and Renewable Sulfur-Polymers by Inverse Vulcanisation, and Their Potential for Mercury Capture. *J. Mater. Chem. A* **2017**, *5* (23), 11682−11692.
(31) Thielke, M. W.; Bultema, L. A.; Brauer, D. D.; Richter, B.; Fischer, M.; Theato, P. Rapid Mercury(II) Removal by Electrospun Sulfur Copolymers. *Polymers (Basel).* **2016**, *8* (7), 266.
(32) Chalker, J.; Mann, M.; Worthington, M.; Esdaile, L. Polymers Made by Inverse Vulcanization for Use as Mercury Sorbents. *Org. Mater.* **2021**, *03*, 362−373.
(33) Wu, X.; Smith, J. A.; Petcher, S.; Zhang, B.; Parker, D. J.; Griffin, J. M.; Hasell, T. Catalytic Inverse Vulcanization. *Nat. Commun.* **2019**, *10* (1), 647.
(34) Worthington, M. J. H.; Mann, M.; Muhti, I. Y.; Tikoalu, A. D.; Gibson, C. T.; Jia, Z.; Miller, A. D.; Chalker, J. M. Modelling Mercury Sorption of a Polysulfide Coating Made from Sulfur and Limonene. *Phys. Chem. Chem. Phys.* **2022**, *24* (20), 12363−12373.
(35) Ghumman, A. S. M.; Shamsuddin, R.; Abbasi, A.; Ahmad, M.; Yoshida, Y.; Sami, A.; Almohamadi, H. The Predictive Machine Learning Model of a Hydrated Inverse Vulcanized Copolymer for Effective Mercury Sequestration from Wastewater. *Sci. Total Environ.* **2024**, *908*, 168034.
(36) Nayeem, A.; Ali, M. F.; Shariffuddin, J. H. The Recent Development of Inverse Vulcanized Polysulfide as an Alternative Adsorbent for Heavy Metal Removal in Wastewater. *Environ. Res.* **2023**, *216*, 114306.
(37) Omeir, M. Y.; Wadi, V. S.; Alhassan, S. M. Inverse Vulcanized Sulfur-Cycloalkene Copolymers: Effect of Ring Size and Unsaturation on Thermal Properties. *Mater. Lett.* **2020**, *259*, 126887.
(38) Limjuco, L. A.; Nisola, G. M.; Parohinog, K. J.; Valdehuesa, K. N. G.; Lee, S. P.; Kim, H.; Chung, W. J. Water-Insoluble Hydrophilic Polysulfides as Microfibrous Composites towards Highly Effective and Practical Hg2+ Capture. *Chem. Eng. J.* **2019**, *378*, 122216.
(39) Eder, M. L.; Call, C. B.; Jenkins, C. L. Utilizing Reclaimed Petroleum Waste to Synthesize Water-Soluble Polysulfides for Selective Heavy Metal Binding and Detection. *ACS Appl. Polym. Mater.* **2022**, *4* (2), 1110−1116.
(40) Wang, M.; Qu, R.; Sun, C.; Yin, P.; Chen, H. Dynamic Adsorption Behavior and Mechanism of Transition Metal Ions on Silica Gels Functionalized with Hydroxyl- or Amino-Terminated Polyamines. *Chem. Eng. J.* **2013**, *221*, 264−274.
(41) Ghumman, A. S. M.; Nasef, M. M.; Shamsuddin, M. R.; Abbasi, A. Evaluation of Properties of Sulfur-Based Polymers Obtained by Inverse Vulcanization: Techniques and Challenges. *Polym. Polym. Compos.* **2021**, *29*, 1333−1352.
(42) Ghumman, A. S. M.; Shamsuddin, R.; Nasef, M. M.; Nisa Yahya, W. Z.; Abbasi, A. Optimization of Synthesis of Inverse

https://doi.org/10.1021/acsomega.3c08361
ACS Omega 2024, 9, 4831−4840

Vulcanized Copolymers from Rubber Seed Oil Using Response Surface Methodology. *Polymer (Guildf).* **2021**, *219*, 123553.
(43) Thommes, M.; Kaneko, K.; Neimark, A. V.; Olivier, J. P.; Rodriguez-Reinoso, F.; Rouquerol, J.; Sing, K. S. W. Physisorption of Gases, with Special Reference to the Evaluation of Surface Area and Pore Size Distribution (IUPAC Technical Report). *Pure Appl. Chem.* **2015**, *87* (9−10), 1051−1069.

https://doi.org/10.1021/acsomega.3c08361
ACS Omega 2024, 9, 4831−4840